CEBAF Program Advisory Committee Eight Cover Sheet

This proposal must be received by close of business on Thursday, April 14, 1994 at:

CEBAF
User Liaison Office, Mail Stop 12 B
12000 Jefferson Avenue
Newport News, VA 23606

Proposal Title

High Q^2 measurement of the ratio of the electric and magnetic form factors of the neutron with polarized ^{3}He using the HRS spectrometers

Contact Person

F. W. Hersman
University of New Hampshire
Department of Physics
Durham, NH 03824
Office: (603)868-6362 FAX: (603) 868-2998
email: hersman@unh.edu

Experimental Hall:	Hall A
Total Days Requested for Approval:	30 days
Minimum and Maximum Beam Energies (GeV):	0.8 GeV $\rightarrow$ 3.2 GeV
Minimum and Maximum Beam Currents (μAmps):	25 μA

CEBAF Use Only

Receipt Date: _____

By: _____

HAZARD IDENTIFICATION CHECKLIST

CEBAF Experiment: 94-006 '4 Date: 5/26/94

Check all items for which there is an anticipated need—do not check items that are part of the CEBAF standard experiment (HRSE, HRSH, CLAS, HMS, SOS in standard configurations).

Cryogenics ____ beamline magnets ____ analysis magnets ____ target ____ drift chambers ____ other	**Electrical Equipment** ____ cryo/electrical devices ____ capacitor banks ____ high voltage ____ exposed equipment	**Radioactive/Hazardous Materials** List any radioactive or hazadorous/ toxic materials planned for use: ____ ____
Pressure Vessels ✓ 0.5 cm inside diameter 10 bar operating pressure glass window material 20 μm window thickness	**Flammable Gas or Liquids** (incl. target) type: ____ flow rate: ____ capacity: ____	**Other Target Materials** ___ Beryllium (Be) ___ Lithium (Li) ___ Mercury (Hg) ___ Lead (Pb) ___ Tungsten (W) ___ Uranium (U) ___ Other (list below) ____ ____
Vacuum Vessels ____ inside diameter ____ operating pressure ____ window material ____ window thickness	**Radioactive Sources** ____ permanent installation ____ temporary use type: ____ strength: ____	**Large Mech. Structure/System** ____ lifting devices ____ motion controllers ____ scaffolding or elevated platforms ____ other neutron detector + shield
Lasers type: Ar+ ; Ti:Saph wattage: 30 ; 6 class: ____ ; ____ **Installation** ____ permanent ✓ temporary **Use** ____ calibration ____ alignment	**Hazardous Materials** ____ cyanide plating materials ____ scintillation oil (from) ____ PCBs ____ methane ____ TMAE ____ TEA ____ photographic developers ____ other (list below) ____ ____ ____	**Notes:** ____ ____ ____ ____ ____ ____

High Q^2 measurement of the ratio of the electric and magnetic form factors of the neutron with polarized ^{3}He using the HRS spectrometers

F. W. Hersman, L. C. Balling, V. Boykin, J. Calarco, J. Distelbrink,
L. Gelinas, J. Heisenberg, M. Kennedy, V. Pomeroy,
Timothy P. Smith, I. The, A. Tutein, J. Wright
University of New Hampshire

M. B. Leuschner
Indiana University

B. Wojtsekhowski
RPI

J.-P. Chen
MIT

O. K. Baker, T. Eden, R. Madey, L. Tang
Hampton University

B. Anderson, L. R. Baldwin, A. Lai, R. Madey, D. M. Manley,
R. Sulieman, J. Watson, W. M. Zhang
Kent State University

currently seeking endorsement of the Hall A Collaboration

F. W. Hersman, contact person

ABSTRACT

We propose to measure polarization observables of $^3\overrightarrow{\mathrm{He}}(\vec{e},e'n)$ in the quasielastic region to extract the neutron electric to magnetic form factor ratio (G_E^n/G_M^n). We plan to use the HRS spectrometers and large arrays of scintillation detectors to detect electrons and neutrons on both sides of the beam line. The high density target is based on existing techniques for polarizing helium by alkali spin exchange. Two beam-target asymmetries in the scattering plane and the normal target asymmetry are all measured to control systematic uncertainties. The anticipated relative precisions in the form factor ratio (2%, 6% and 17%) correspond to uncertainties of 0.0011 in G_E^n at 0.51 GeV/c^2, and approximately 0.0015 at 1.38 and 3.37 GeV/c^2.

1. Introduction

The neutron electric form factor has been the subject of considerable theoretical and experimental investigation. Because the main component of the nucleon wave function is symmetric, the structure is directly sensitive to small admixtures in the wave function due to the negative pion cloud, color magnetic forces[1] or higher order diagrams in QCD, presumably at different values of momentum transfer. While the neutron charge radius has been measured by scattering free neutrons from electrons, higher momentum transfer measurements must be performed using lepton beams on neutrons bound in nuclei. Deuterium and ^{3}He are the natural choices. Due to the fundamental importance of neutron properties, the possibility of form factor medium modifications due to binding, and the substantial differences in the technologies available for the targets, measurements from neutrons in both of these nuclei should be performed.

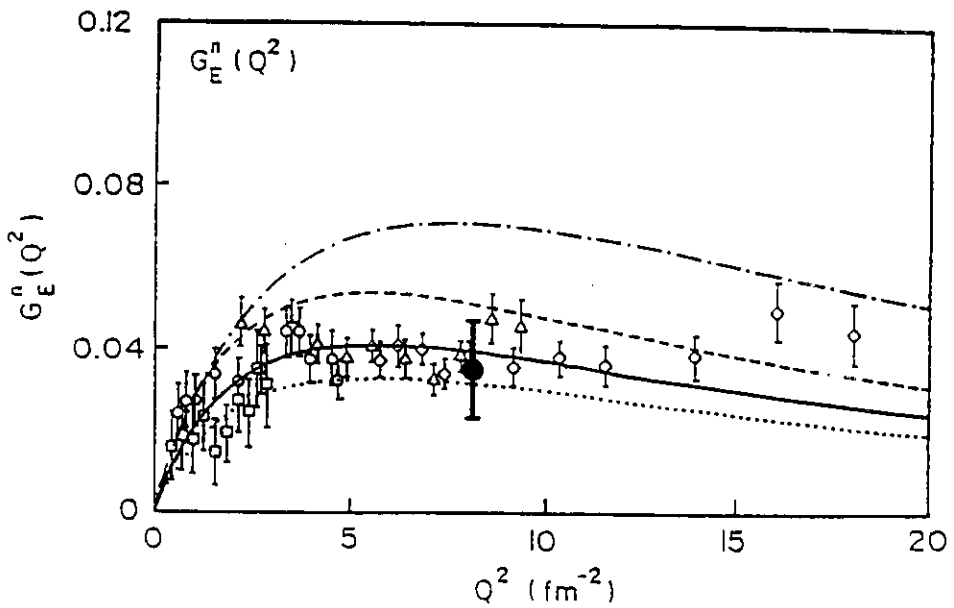

Fig. 1. Deuteron elastic charge scattering data plotted as a deviation from the cross section calculated using wave functions given by the Paris potential. A parametrization of the neutron electric form factor that provides agreement with the data is indicated by the solid line. A direct measurement of G_E^n extracted from polarized $^3\overline{\mathrm{He}}(\vec{e},e'n)$ from Mainz is indicated by the large data point.

Previous extractions of the neutron form factor from unpolarized measurements have been model dependent or insensitive. Precision measurements of the deuteron electric form factor have been analyzed in the context of wave functions derived from non-relativistic potential models,[2,3] providing a best fit with a positive value of the

form factor, G_E^n around 0.04 in the vicinity of 0.5 GeV/c^2. A Rosenbluth separation of quasielastic electron scattering from deuterium performed recently[4] gave values of $(G_E^n)^2$ consistent with zero. The error bars were also consistent with most credible theories.

Polarization observables enhance the sensitivity to small components of nucleon structure. Polarized ^{3}He provides, to a good approximation, a target of highly polarized neutrons with an almost unpolarized proton background. Coincidence $(\vec{e},e'n)$ measurements can be used to identify the struck nucleon as a neutron, and remove the proton background. The formalism of electron scattering from free neutrons is presented in Chapter 2.

Several groups have developed proposals to measure quantities related to the neutron electric form factor with polarized electrons and polarized ^{3}He. Experiments to perform inclusive scattering measurements on ^{3}He have been performed,[5,6] and continue at the MIT-Bates accelerator. A plan by MIT, Caltech and others[7] to extend these measurements to internal targets using the Bates Large Acceptance Spectrometer Toroid (BLAST) is approved. These proponents also describe[8] an inclusive scattering measurement using CLAS to extract G_E^n, currently conditionally approved.

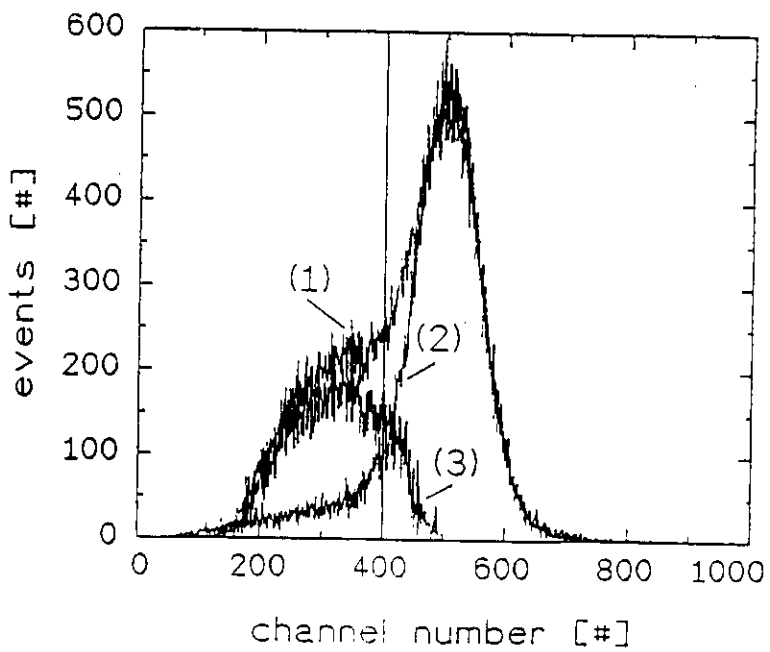

Fig. 2. Electron spectrum measured in lead glass detectors at Mainz associated with coincidence (e,e'n) events. Events associated with Δ production limit the precision.

The A3 collaboration [9] at Mainz adopts a different strategy. By basing the measurement on exclusive (e,e′n) they suppress much of the model dependence and the dilution associated with scattering from the protons in ^{3}He. A large acceptance Pb glass wall and an air Čerenkov detector identify electrons while a scintillator wall measures neutron time-of-flight. A first measurement of G_E^n was recently extracted from their measured asymmetries. (Fig. 1) Improvements in the detector acceptances and target density will significantly reduce the statistical uncertainty. Systematic effects associated with insufficient electron energy resolution to exclude pion production channels contribute 10% to the systematic uncertainty (Fig. 2).

We propose to measure the polarization response of $^3\overrightarrow{\mathrm{He}}(\vec{e},e'n)$ in the quasielastic region. The primary goal of this measurement is to extract the ratio of the neutron electric to magnetic form factor to high momentum transfer. Measuring two points of the angular distribution of the asymmetry simultaneously reduces the experimental systematic uncertainty. The kinematics where the target polarization is nearly perpendicular to the momentum transfer provides a measurement of the ratio of G_E^n/G_M^n that is insensitive to the polarization of the beam and target, even insensitive to the fractional polarization of the neutron in the ^{3}He wave function. The kinematics where the target polarization is nearly parallel to the momentum transfer provides an asymmetry measurement that depends principally on the beam and target polarization (and kinematic factors). Measurement of the normal asymmetry, A_y^0, which vanishes in impulse approximation, provides a benchmark calibration of higher order processes. This measurement helps to control "theoretical systematic uncertainty". We propose to measure the three nonvanishing asymmetries at Q^2=0.51, 1.38, and 3.38 GeV/c^2.

We have fabricated a prototype high pressure, polarized ^{3}He target based on the alkali spin exchange technique already in use at several laboratories. The most significant new features of our target are its small volume and thin windows. The details of the target are presented in Chapter 3. We also describe in that chapter the neutron detection apparatus and its particle identification and shielding requirements.

In Chapter 4 we present the plan for the measurement. We first describe the selected kinematics of the quasielastic $^3\overrightarrow{\mathrm{He}}(\vec{e},e'n)$ measurements. We calculate the counting rates and asymmetries using Monte Carlo simulations including detector acceptances and efficiencies. We then estimate the statistical and systematic precision of the extracted ratio of G_E^n/G_M^n (translated into an uncertainty in G_E^n). We request 30 days.

2. Quasielastic scattering from a polarized $^3\overrightarrow{\mathrm{He}}$ target

The cross section for the inclusive scattering of longitudinally polarized electrons from a polarized target is:[10,11]

$$\frac{d\sigma}{d\Omega d\omega} = \Sigma \pm \Delta(\theta^*, \phi^*)$$

where θ^* and ϕ^* is the spin direction of the target relative to the momentum transfer $\vec{q}$ vector and the plane of the electron scattering. The $\pm$ corresponds to the helicity of the incident electron. The spin independent and spin dependent terms are:

$$\Sigma = 4\pi\sigma_{\mathrm{M}} f^{-1}[v_L R_L + v_T R_T]$$
$$\Delta = -4\pi\sigma_{\mathrm{M}} f^{-1}[\cos\theta^* v_{T'} R_{T'} + 2\sin\theta^* \cos\phi^* v_{TL'} R_{TL'}]$$

where the response functions R_L, R_T, $R_{T'}$, and $R_{TL'}$ depend on the four-momentum transfer $Q^2 = q^2 - \omega^2 > 0$. The Mott cross section σ_{M}, the recoil factor f, and the kinematic factors v's are given by

$$\sigma_{\mathrm{M}} = \frac{\alpha^2 \cos^2(\theta_e/2)}{4E_0^2 \sin^4(\theta_e/2)}$$
$$f = 1 + \frac{2E_0}{M}\sin^2\frac{\theta_e}{2}$$
$$v_L = \left(\frac{Q^2}{q^2}\right)^2$$
$$v_T = \frac{1}{2}\left(\frac{Q^2}{q^2}\right) + \tan^2\frac{\theta_e}{2}$$
$$v_{T'} = \tan\frac{\theta_e}{2}\sqrt{\left(\frac{Q^2}{q^2}\right) + \tan^2\frac{\theta_e}{2}}$$
$$v_{TL'} = -\frac{1}{\sqrt{2}}\left(\frac{Q^2}{q^2}\right)\tan\frac{\theta_e}{2}$$

α, E_0, M, and θ_e are the fine structure constant, the incident electron energy, the target mass (the neutron mass in this case), and the electron scattering angle, respectively.

For the specific case of electrons scattering from polarized (free) neutrons, the spin independent and dependent parts are written:

$$\Sigma = \sigma_M f^{-1}[v_L(1+\tau)^2(G_E^n)^2 + 2\tau(1+\tau)v_T(G_M^n)^2]$$
$$\Delta = -\sigma_M f^{-1}[2\tau(1+\tau)v_{T'}\cos\theta^*(G_M^n)^2 - 2(1+\tau)\sqrt{2\tau(1+\tau)}v_{TL'}\sin\theta^*\cos\phi^* G_M^n G_E^n]$$

where $\tau = Q^2/4M^2$.

A measurement with the momentum transfer $\vec{q}$ direction parallel to the target spin maximizes sensitivity to R_T', while a measurement with $\vec{q}$ perpendicular to the target spin accesses the response function $R_{LT'}'$ proportional to G_E^n. It can be shown, however, that the asymmetry (Δ/Σ) is sensitive only to the ratio of G_E/G_M by dividing Δ by Σ and factoring out the common $(G_M^n)^2$. The asymmetry is revealed as a function of a single physical quantity, G_E^n/G_M^n and kinematic factors. Setting $g = G_E^n/G_M^n$ gives

$$A = \frac{\Delta}{\Sigma} = -\frac{2\tau v_{T'}\cos\theta^* - 2\sqrt{2\tau(1+\tau)}v_{TL'}\sin\theta^*\cos\phi^* g}{v_L(1+\tau)g^2 + 2\tau v_T}$$

Neglecting (for demonstration purposes) the term proportional to g^2, we get:

$$A_{\rm exp} = p_e p_n(k_1\cos\theta^* + k_2\sin\theta^*\cos\phi^* g)$$

where p_e and p_n are the electron and neutron polarizations and k_1 and k_2 are trivial kinematic factors.

The angular distribution of the asymmetry in the region with the $\vec{q}$ direction perpendicular to the target spin provides a good measure of G_E^n/G_M^n. Location of the kinematics where the asymmetry vanishes, for example, provides substantial sensitivity to G_E^n/G_M^n but with no sensitivity to the beam and target polarization.[12] Conversely the dominant term in the parallel asymmetry depends on kinematic factors and the beam and target polarization, providing a continuous polarization monitor. Our choice of target angles emphasizes determination of the zero asymmetry kinematic region in one of the HRS spectrometers, while the other measures a large asymmetry that is nearly independent of G_E^n/G_M^n.

3. Experimental Details

3.1 Target

The target technology we have selected for this measurement has been developed over the past 8-10 years by the Princeton group.[13] and used in several measurements at several laboratories. The high density and high polarization offered by this technology provides an excellent figure of merit for studies where maximum density is important. It has already been used very successfully for a deep inelastic scattering measurement at SLAC that had target requirements similar to ours. Furthermore, refinements of this technology continue to offer improvements in performance. It is appropriate to mention that an alternative technology is being pursued at Mainz in which helium nuclei are polarized by metastability exchange and compressed. This technology has also provided excellent performance and offers further improvements as well. We discuss below our plans in terms of the SLAC spin exchange target parameters, and outline briefly our program for improvements.

We will use a ^{3}He target pressurized to 10 atmospheres of helium, or $2.7\times10^{20}/\mathrm{cm}^3$ over a length of 15 cm, for a total thickness of $4\times10^{21}/\mathrm{cm}^2$ or 20 mg/cm^2. A beam current of 25 μA (1.5×10^{14}) will provide a luminosity of 6×10^{35} electron-^{3}He/cm^{2}sec. The extended target acceptance of the HRS of 10 cm allows essentially all of the target to be viewed at the relevant scattering angles between 50° and 70°. A new concave inward design for the window[14] has been developed at UNH and tested at 5 atmospheres without beam. In-beam tests are planned at Bates. It may be kept in mind that if beam related failures of the glass window under high pressure becomes a concern, the target cell may be placed in an environment pressurized to 10 atmospheres without substantial difficulty.

The ^{3}He target is polarized by optically pumping an alkali metal vapor (rubidium) which spin exchanges with helium. Circularly polarized light of 795 nm (the D_1 line) is absorbed by s-shell electrons with the opposite spin, promoting them to the $p_{1/2}$-shell. Subsequent collisions with helium and nitrogen mix the p-shell polarization and promote nonradiative decays to the ground state, with equal probability for each spin state. The depletion of one spin state leads to accumulation of rubidium atomic polarization. Polarization is transferred to helium nuclei through the hyperfine interaction during collisions.

The design uses two cells, a pumping cell and a target cell. The pumping cell is maintained at elevated temperature, adjusted to control the rubidium vapor pressure. It is located 5 cm off-axis and at an angle of 55° with respect to the beam. It must

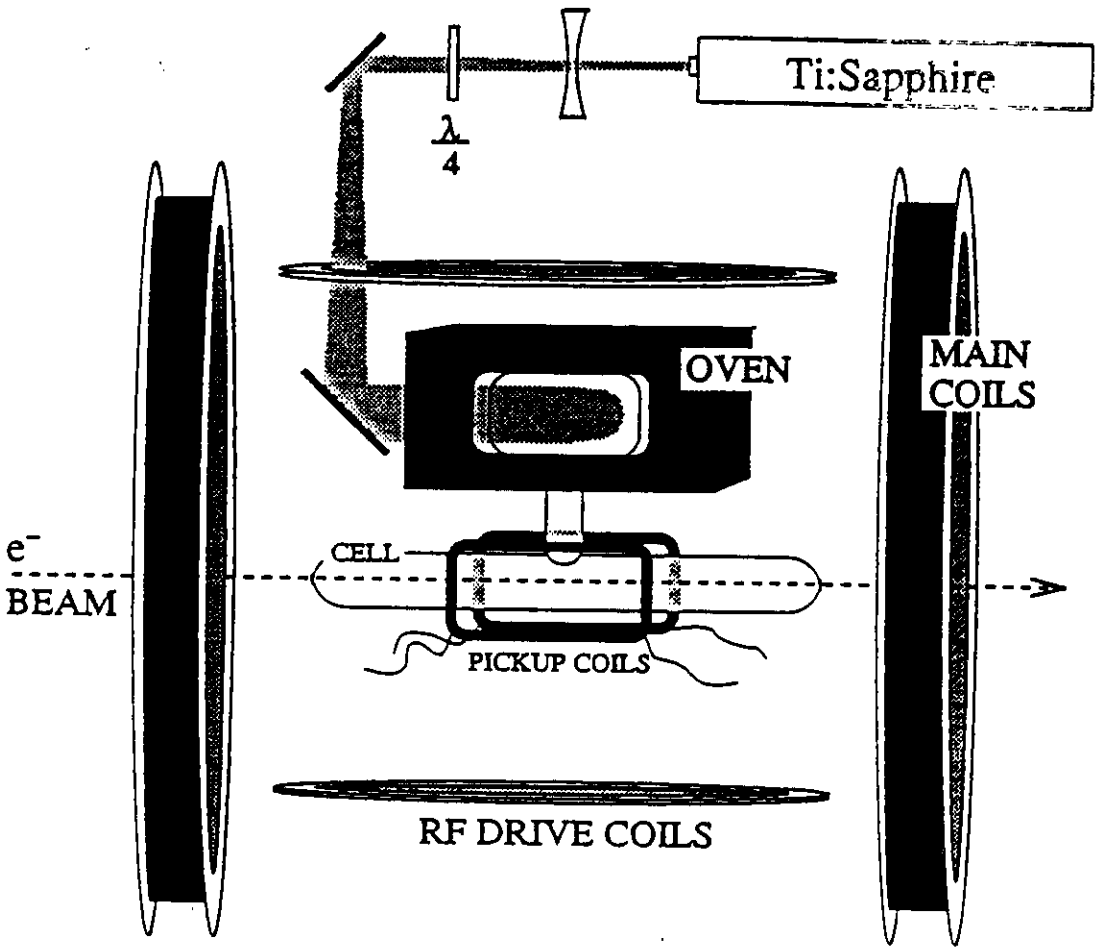

Fig. 3 The SLAC E142 alkali spin exchange helium target.[15,16] The target design we propose differs only in the cell diameters and the window design.

be fully illuminated to maximize the polarization. The target cell is held at a lower temperature to assure that the rubidium plates out on the transfer tube and does not enter the target cell. (Fig. 3) Target polarization is measured by adiabatic fast passage nuclear magnetic resonance. An integrated measure of beam polarization times neutron polarization is extracted from one of the scattering asymmetries.

Coincidence quasielastic scattering from neutrons in 100 torr of nitrogen contributes a 14% dilution over the volume of the cell. Coincidences from scattering off of neutrons in the glass windows can be eliminated by electron track reconstruction. Scattering from nitrogen is measured with an equivalent target of the same geometry (with additional nitrogen) and subtracted. While remaining uncertainties in this dilution contribute to uncertainties in the cross section, they do not contribute to uncertainties in the extracted ratio of electric to magnetic form factor. We continue seeking design possibilities that reduce the nitrogen thickness. We are considering the use of ^{15}N to remove any question of partial neutron polarization arising from any nitrogen polarization.

The largest source of rubidium depolarization is wall contact, which must be overcome with laser intensity. We intend to maximize the polarization by reducing the diameter of the pumping cell, minimizing the surface area and concentrating the laser power. A simple analysis indicates that significantly higher rubidium densities can be pumped at fixed laser power, leading to substantially faster polarization rates. While we use the parameters of the SLAC target for our estimates, we intend to develop a target with pumping cell and target cell diameters of 5 mm. First prototype tests are underway.

3.2 Magnetic fields

The quantization axis is provided by a set of Helmholtz coils. The diameter is chosen as large as possible to provide a maximally uniform field, while maintaining clearance from the quadrupoles Q1 in the forward position at 90 cm. We choose a radius of 60 cm. A slightly larger Helmholtz pair is oriented perpendicular to the first. This coil set will be used for slow polarization rotation and reversal, and also for providing the quantization axis during adiabatic fast passage nuclear magnetic resonance (the polarization will be measured in a different orientation than the data taking to simplify the pickup coil design).

The magnetic field from Q1 in the vicinity of the target reaches a maximum on order of 1 gauss. We intend to suppress stray magnetic fields from the quadrupoles Q1 using a field clamp. We are planning to study the effectiveness of a "doughnut" shaped iron plate mounted 15 cm from the quadrupole aperture in providing a return path for stray

flux. If necessary a similar sheet of mu-metal will be added a short distance in front of the plate.

The angle of the quantization axis is slightly different for the three measurements, ranging from 42.83° at the lowest momentum transfer to 57.75° at the highest momentum transfer. Since the glassware requires a single photon polarization axis (chosen at 55°), a 2.3% loss of polarization at the lowest momentum transfer will be due to this misalignment.

Magnetic fields associated with the beam current are of little significance to depolarization since the repetition rate is far from resonance with the Larmor precession of the nuclei.

3.3 Neutron detection

Neutron detection is performed by scintillation detectors. Twenty existing fully instrumented neutron detectors 1 m by 1/2 m by 10 cm will be provided by the Hampton group. Requests for additional detectors have been submitted to the funding agency. We have designed our measurement around two stacks of such scintillators, one of them 4 by 4 to form a detector 1 m by 2 m by 40 cm to measure the parallel asymmetry, and one of the 6 by 4 to form a detector 1 m by 2 m by 60 cm to measure the perpendicular asymmetry. Each stack will be preceded by 4 veto detectors identical in planar dimensions but only 1-2 cm thick. A total of 40 thick detectors and 8 thin detectors are planned. A potential neutron detection efficiency (without shielding) of 47% is possible. We assume transmission of 80% through the shielding, yielding total neutron detection efficiency of 37%. (Fig. 4)

The dimensions of the neutron detectors were optimized using the Monte Carlo program MCEEP.[17] The acceptance of the neutron detectors was varied by trial and error, and the rates calculated by MCEEP were compared. The acceptance which gave about 90% of the maximum rate were chosen to keep the size of the neutron detectors within reasonable limits. A solid angle of 300 mr (horizontal) and 600 mr (vertical) satisfied this criterion, determining the aspect ratio of the stack mention above. The detector stack will be placed 4.25 m from the target.

GEANT simulations have been performed to study the forward shielding requirements of the neutron detectors. These simulations identify Moller electrons as the principle contribution to the background rate. A forward shield of low-Z material was shown to eliminate these electrons by multiple scattering while preserving the neutron flux more effectively than a high Z material (by radiation).

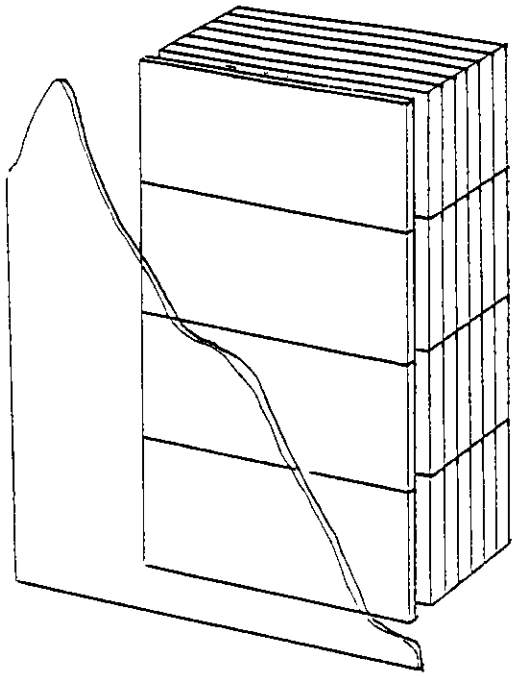

Fig. 4. Diagram of the neutron detector to be used in the measurement, including the front shield and charged particle veto.

Considerable experience exists within the proponents of this measurement on the design and installation of shielding of non-focusing detectors. In fact the lack of substantial and versatile shielding resources within Hall A has been identified by the Hall A Collaboration as a concern. Through simulations and beam tests, this collaboration will work closely with CEBAF staff and engineers in designing specific shielding issues related to this measurement, as well as addressing general shielding issues for nonfocusing detectors in Hall A.

3.4 Beam polarization

A high current high polarization photocathode will be used for this experiment, providing 75% beam polarization. Condensed matter researchers at New Hampshire are preparing to contribute to the development and fabrication of reliable high efficiency photocathodes. Beam polarization will be measured by Møller polarimetry, to a precision of approximately 3%. This uncertainty does not contribute significantly to the final result.

4. Plan for measurement of quasielastic asymmetries to extract G_E^n/G_M^n

We describe our plans to measure quasielastic asymmetries in $^3\overrightarrow{He}(\vec{e},e'n)$ to determine the ratio of the neutron electric to magnetic form factor. Three asymmetries are measured, two of them simultaneously. The first asymmetry is chosen at kinematics where the asymmetry nearly vanishes, but the theoretical dependence of the asymmetry on the neutron electric form factor is a maximum. This asymmetry is close to the "perpendicular asymmetry." (Fig. 5) The second asymmetry is measured near where the theoretical dependence of the asymmetry on G_E^n vanishes, but the asymmetry is large and depends on kinematic factors. This asymmetry is close to the "parallel asymmetry," and is measured simultaneously with the first. Finally the normal target asymmetry A_y^0 is measured separately, providing a calibration of the final state interactions and meson exchange currents. (Fig. 6) Measurement of this asymmetry uses only 2.5 days, but may be critical in interpreting the other measurements at a high level of precision.

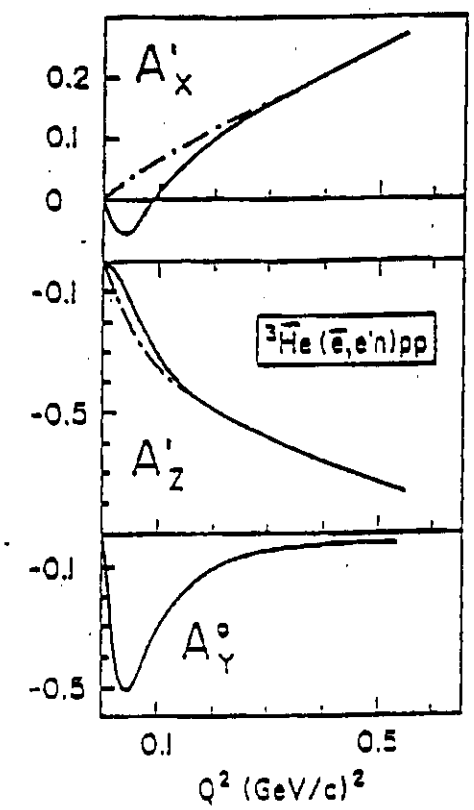

Fig. 6. Final state interactions and meson exchange currents can modify the impulse approximation description of the quasifree asymmetries, particularly at low momentum transfers. Measurement of the normal asymmetry provides a calibration of theoretical corrections.[18]

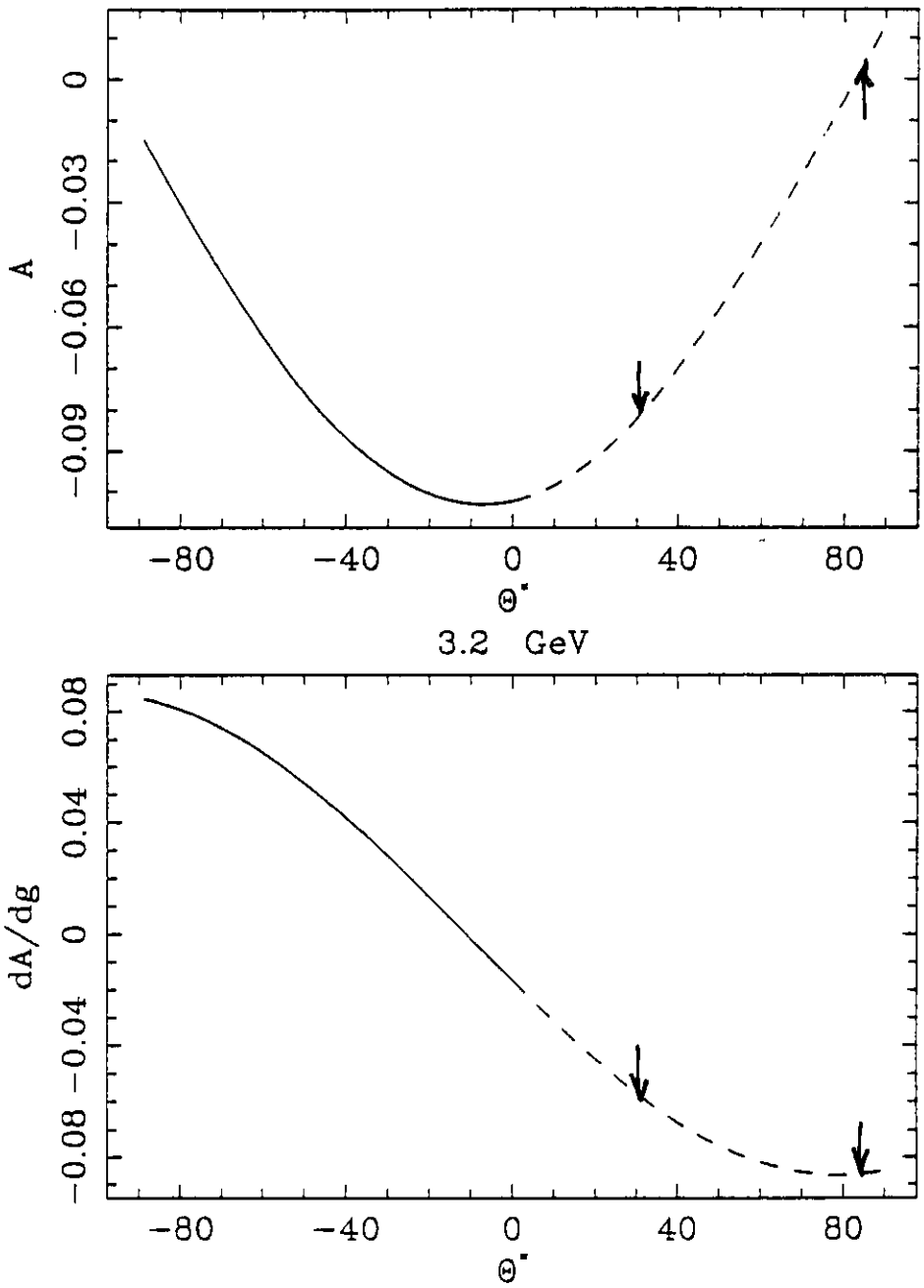

Fig. 5 Kinematics for the measurement at Q^2=3.4 GeV/c^2. The asymmetry and the derivative of the asymmetry with respect to g are plotted against laboratory angles for both sides of the beam line. Arrows indicate the selected kinematics.

4.1 Kinematics

We choose three sets of kinematic parameters for this measurement. (Fig. 7) The lowest Q^2 at 0.5 GeV/c^2 provides a high statistical precision kinematics to compare with previous measurements, to check out the instrumentation, and to explore various cuts on the data. The two high momentum transfer points provide excellent statistical and systematic precision for $Q^2 = 1.4$ and 3.4 GeV/c^2. The normal asymmetry A_y^0 is measured for the lower two kinematics only.

The requirement to measure two exclusive asymmetries simultaneously place constraints on these choices. Both sides of the beam line have spectrometers and neutron detectors. The spectrometers and neutron detectors are placed symmetrically in quasifree kinematics chosen to minimize the angle between them. This choice minimizes the momentum transfer and maximizes count rate for each choice of beam energy.

TABLE 1

Kinematics for asymmetry measurements (GeV)

E_0	Q^2	$\vec{q}$	ω	$\theta_{e'}$	θ_q	θ_S
0.8	0.51	0.763	0.271	66.48°	39.48°	42.83°
1.6	1.38	1.384	0.733	59.77°	32.77°	49.19°
3.2	3.38	2.567	1.794	51.29°	25.30°	57.76°

At the highest momentum transfers the Δ production peak and the quasielastic peak merge. (Fig. 8) The missing energy resolution is insufficient to fully discriminate against pion production. It is at these highest momenta where kinematic focusing concentrates the quasifree neutrons into a smaller aperture. Nucleons associated with the Δ production peak are emitted into larger angles. We are examining the possibility of selecting events based on the location of the detected neutrons in the scintillator stack. (Fig. 9)

4.2 Estimated results

We estimated the counting rates using the factorized form for the coincidence cross section for a quasielastic nucleon knockout reaction in PWIA. The coincidence cross section can be expressed as a product of a kinematic factor times the (off-shell) elastic electron-nucleon cross section (σ_{eN}) times a spectral function (momentum distribution

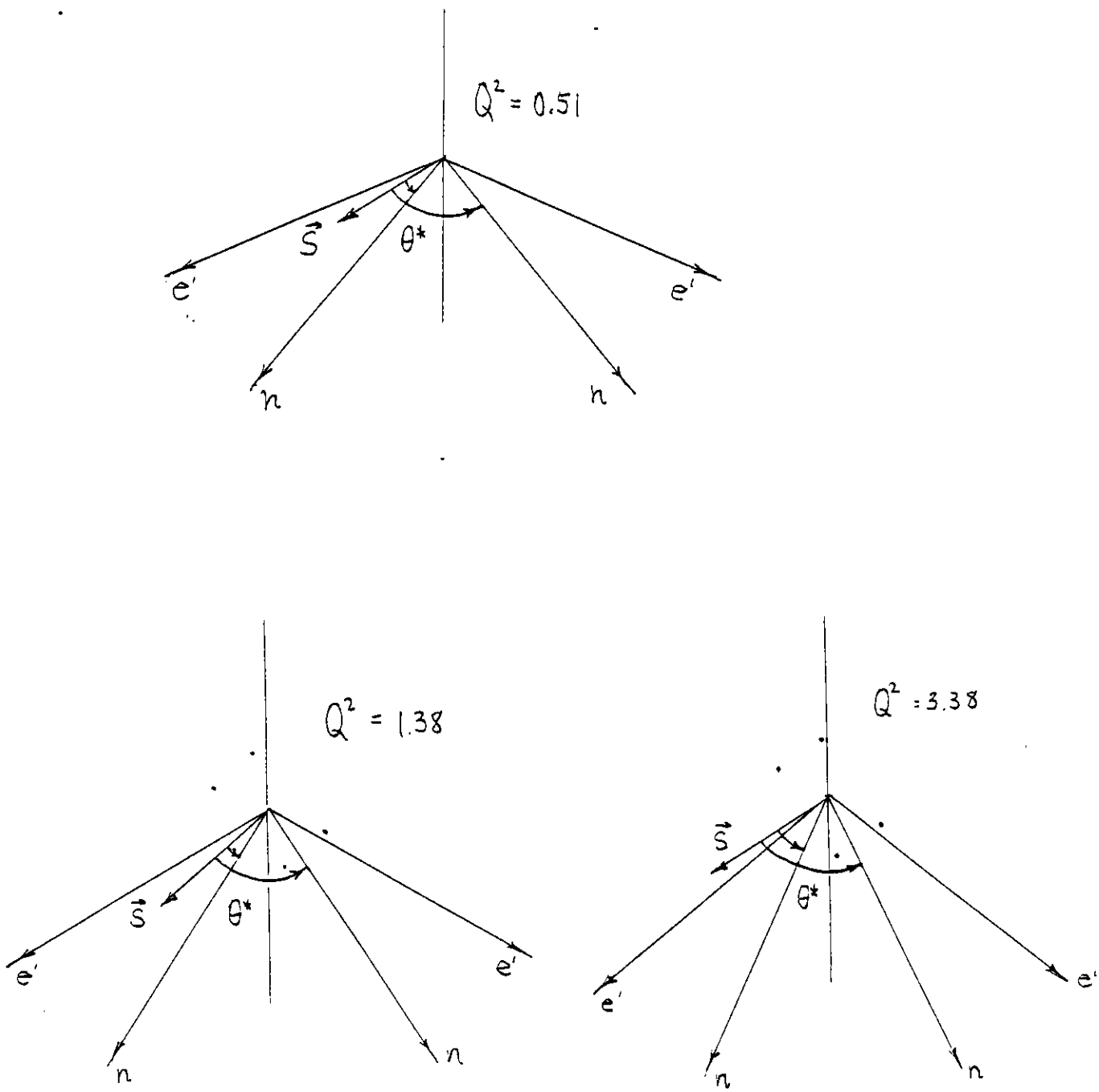

Fig. 7 Kinematics diagrams for the three measurements. The scattering angle, momentum transfer and quantization axis as well as placement of the spectrometers, neutron detectors, and Helmholtz coils are indicated. Suitable gas flow shielding.

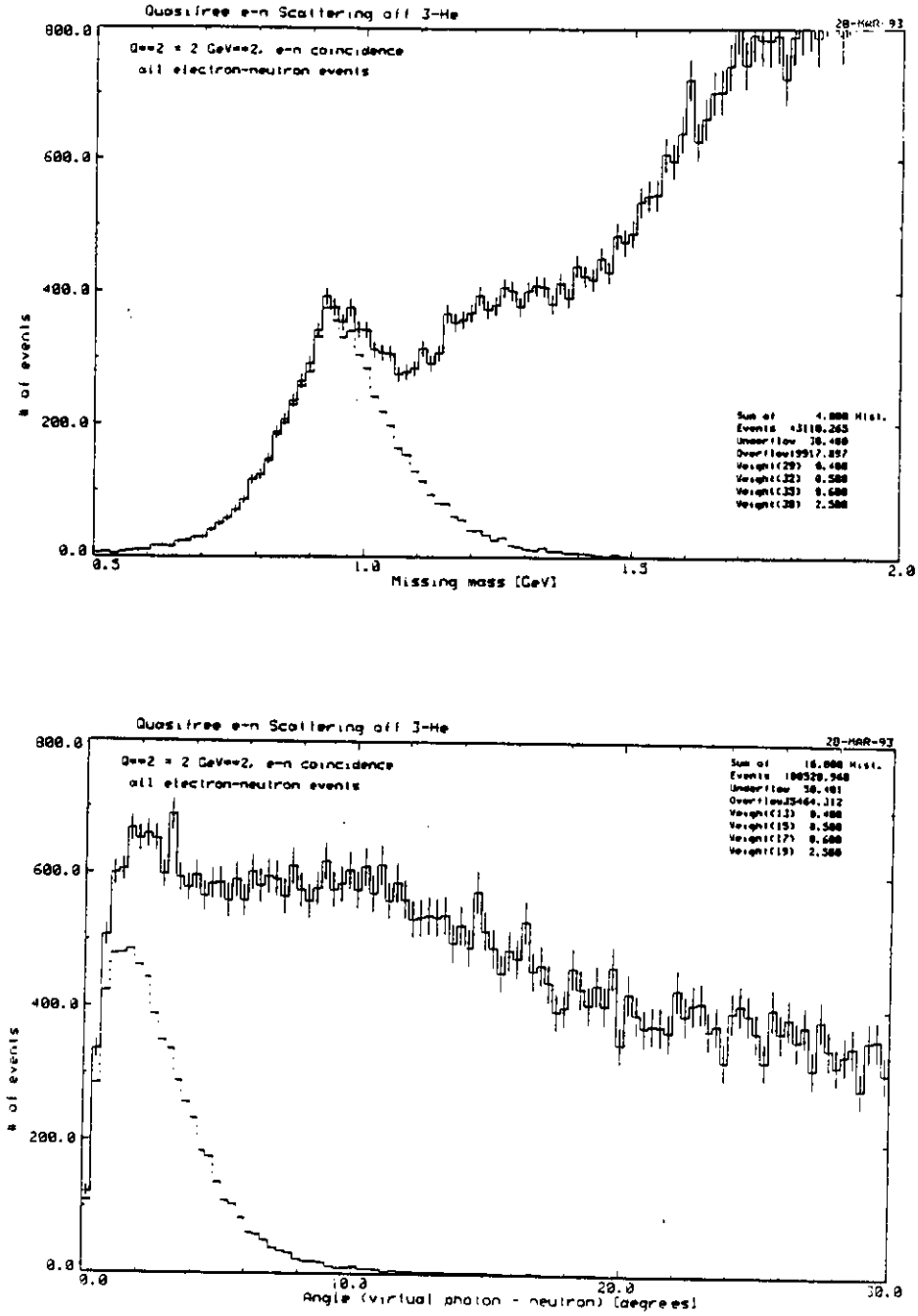

Fig. 8 Quasielastic (e,e'n) events at Q^2=3.0 GeV/c^2 are mixed among the electron kinematics with events from other reaction processes. Most of these events have large neutron angles relative to the momentum transfer.

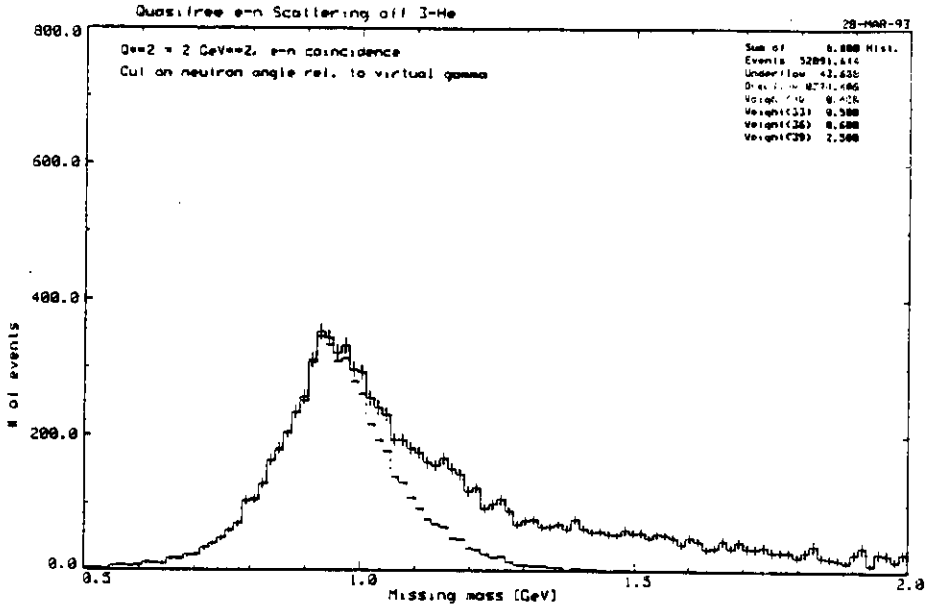

Fig. 9. By performing cuts on the neutron angle at 7°, most of the quasielastic events can be cleanly separated. Cuts on both electron and neutron kinematics provide the best filter.

density ρ)[19] :

$$\frac{d^6\sigma}{de' d\Omega_e d\Omega_N dE_N} = p_N E_N \times \sigma_{eN} \times \rho(p_m, E_m),$$

where p_N and E_N are the momentum and total energy of the recoil nucleon, and p_m and E_m are the missing momentum and missing energy of the unobserved particle. The off-shell electron-neutron cross section is calculated using the "cc1" cross section proposed by de Forest. Losses of 20% of the events due to electron radiation was assumed. A Monte Carlo program MCEEP[17] was used to estimate the coincidence counting rates.

We present counts, asymmetries, and uncertainties for each of three kinematics in Table 2. Asymmetries quoted are based on the Galster model of G_E^n (undiluted by experimental polarizations). Uncertainties are based on a beam polarization of

75% and target polarization of 40% (average neutron polarization of 35%). While the quantity extracted from the measurements is the ratio of G_E^n/G_M^n, the uncertainties are represented as uncertainties in G_E^n (with $G_M^n = \mu_n G_D$, and the dipole form factor $G_D = (1+Q^2/0.71)^{-2}$). Plots of the extracted ratio g as well as these data converted to uncertainties in $G_E^n = -\tau G_M^n/(1+5.6\tau)$ are shown in (Fig. 10) with our estimates of the experimental precision. We request 30 days.

4.3 Institutional commitment

The University of New Hampshire group has had for many years an MOU to design and implement the Hall A trigger for the two HRS spectrometers. John Calarco is leading that effort. The design work is now complete, and the first batch of electronics is being purchased. The UNH group also has a collaborative effort with the UNH Atomic Physics group to fabricate a polarized target for an approved experiment at the Saskatchewan Accelerator Laboratory. We intend to provide a similar target for these measurements.

The Hampton/Kent State University collaborators intend to provide fully instrumented neutron detectors for this measurement. Several counters are presently available and more have been included in their present funding request.

TABLE 2

Counts, physical asymmetries, and uncertainties.

	Q^2	counts	Ay	ΔAy	$\partial A/\partial G_E^n$	ΔG_E^n	G_E^n	days
$A_{\parallel}$	0.51	1,500,000	0	0.0024	2.8	0.0011	0.051	4.0
$A_{\perp}$	0.51	1,000,000	−0.85	0.003	0.94	–	–	–
A_y^0	0.51	500,000	0	0.004	0	–	–	1.0
tests	0.51	500,000	0	0.004	0	–	–	1.0
$A_{\parallel}$	1.38	250,000	0	0.006	5.0	0.0015	0.026	6.6
$A_{\perp}$	1.38	170,000	−0.77	0.007	2.6	–	–	–
A_y^0	1.38	80,000	0	0.011	0	–	–	1.5
tests	1.38	80,000	0	0.011	0	–	–	1.5
$A_{\parallel}$	3.37	42,000	0	0.015	12.4	0.0015	0.0086	14.4
$A_{\perp}$	3.37	28,000	−0.65	0.018	8.6	–	–	–
							TOTAL	30.0

1. Nathan Isgur, Gabriel Karl, and Roman Koniuk, *Phys. Rev.* **D25** (1992) 25.
2. S. Galster, *et al.*, *Nucl. Phys.* **B32** (1971) 221.
3. S. Platchkov, *et al.*, *Nucl. Phys.* **A510** (1990) 740.
4. A. Lung, *et al.*, *Phys. Rev. Lett.* **70** (1993) 718.
5. C. E. Woodward, *et al.*, *Phys. Rev. Lett.* **65** (1990) 698, C. E. Jones-Woodward, *et al.*, *Phys. Rev.* **C44** (1991) R571.
6. A. K. Thompson, *et al.*, *Phys. Rev. Lett.* **68** (1992) 2901.
7. Bates experiment 89-12, J.F.J. van den Brand and R. G. Milner, spokesmen (1990).
8. CEBAF Proposal 91-020, R. McKeown, spokesman.
9. M. Myerhoff, *et al.*to be published.
10. B. Blankleider and R. M. Woloshyn *Phys. Rev.* **C29** (1984) 558.

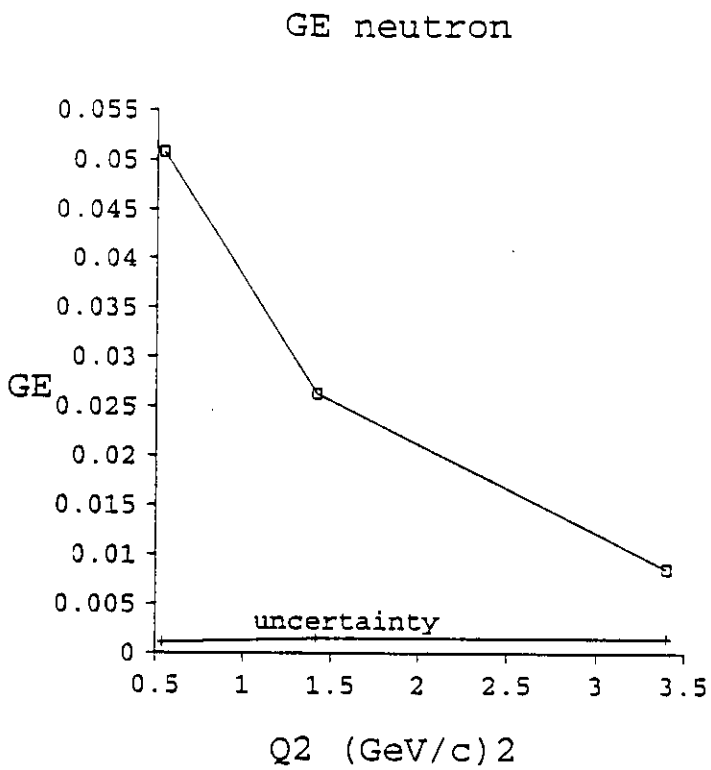

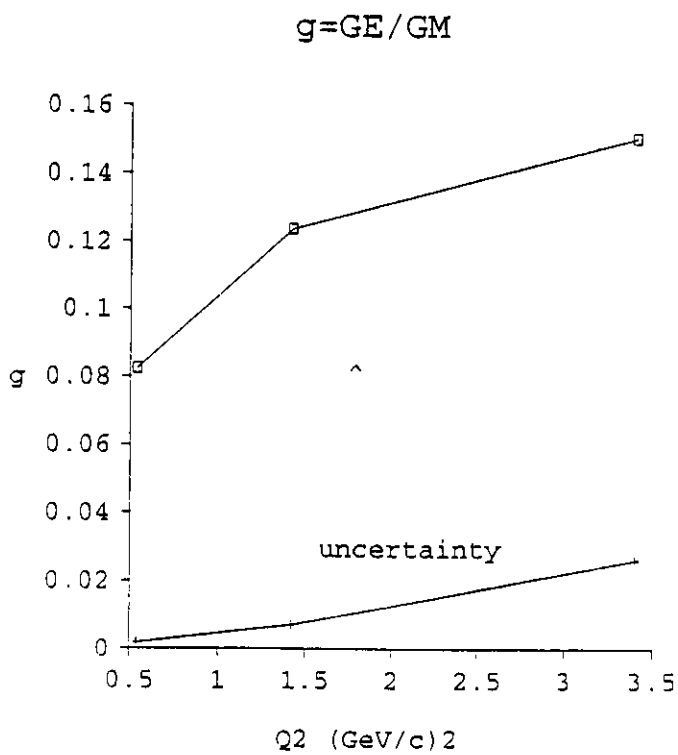

Fig. 10 A model of $g = G_E^n/G_M^n$ and [illegible] with the estimate of the experimental uncertainty.

11. C. Woodward, Ph.D. thesis, Caltech.

12. B. A. Mecking, private communication.

13. T. E. Chupp, *et al.*, *Phys. Rev.* **C45** (1992) 915 and references therein.

14. F. W. Hersman, Proceedings of the Conference on Polarized Ion Sources and Polarized Gas Targets, Madison, WI (1993)

15. H. Middleton, *et al.*, Proceedings of the Conference on Polarized Ion Sources and Polarized Gas Targets, Madison, WI (1993)

16. G. D. Cates, Polarized Targets in High Energy Physics, preprint.

17. P.E. Ulmer, MCEEP: Monte Carlo for Electro-Nuclear Coincidence Experiments, version 1.01 (1991).

18. J. M. Laget, *Phys. Lett.* **B273** (1991) 367.

19. T. De Forest, Jr., Nucl. Phys. **A392**, 232 (1983).